PART 2 Historical Mountain Geomorphology

Cascade Mountain, Banff, Alberta, Canada
Photo: P.N. Owens

2
Cenozoic evolution of global mountain systems

Lewis A. Owen

1 Introduction

Mountain systems are among the most prominent geomorphic features on the Earth. Tectonically, they are major belts of pervasive deformation that include thick sequences of shallow-water sandstones, limestones and shales deposited on continental crust, and oceanic deposits characterized by deep-water turbidites and pelagic sediments, commonly with volcaniclastic sediments and volcanic rocks. Typically, mountain systems have been deformed and metamorphosed to varying degrees and intruded by plutonic rocks, chiefly of granitic affinity (Moores and Twiss, 1995).

The geologic evolution of these orogenic belts is complex and may span hundreds of millions of years. During the latter part of the twentieth century the application of plate tectonic theories to the study of orogenic belts revolutionized the understanding of the dynamics and evolution of these systems. Furthermore, the rapid development of geophysical and geochemical techniques has aided the measurement, monitoring and modelling of the evolution of mountain systems on local, regional and global scales. Contemporary research on the evolution of mountain systems involves most branches of geology, particularly geodesy, geophysics, geochemistry, structural geology, sedimentology, stratigraphy, geomorphology and palaeoclimatology (Zeitler *et al*., 2001; Bishop *et al*., 2002).

A casual comparison of topographic and tectonic maps of the world clearly shows that the major high mountain systems occur along or are parallel to lithospheric plate boundaries (Figure 2.1). The majority of these mountain systems began to form and largely evolved during the Cenozoic (~65 Ma to present). These are commonly referred to as 'young' mountain systems and 'active' if they are presently deforming. Of particular note are the Alpine–Himalayan–Tibetan and the Circum-Pacific orogenic systems, and the ocean ridges. Closer inspection reveals regionally extensive and significant mountain belts of lesser relief. These 'ancient' mountain systems generally have little or no relationship to the present lithospheric plate boundaries and may have begun to have formed many hundreds of millions of years ago. Despite their age and distance from plate margins these mountain systems may still experience deformation, albeit not so dramatic as young active mountain belts. Often their major pervasive geologic structures are zones of discontinuity along which earthquakes may occur. The Appalachian–Caledonide system is one of the best examples. This mountain system stretched for some 6000 km and now includes the Caledonides of east Greenland, Svalbard, Ireland, Britain and Scandinavia, the Appalachians of the USA and Canada, the Innuitian Mountains of Arctic Canada and Greenland, the Ouachita Mountains of south-central USA, the Cordillera Oriental in Mexico, the Venezuelan Andes and the West African fold belt. The evolution of this mountain system began in the late Precambrian (>~570 Ma), and the deformation and mountain building occurred during three major orogenies, during the early, middle and late Palaeozoic (between ~570 Ma and ~250 Ma). The mountain system

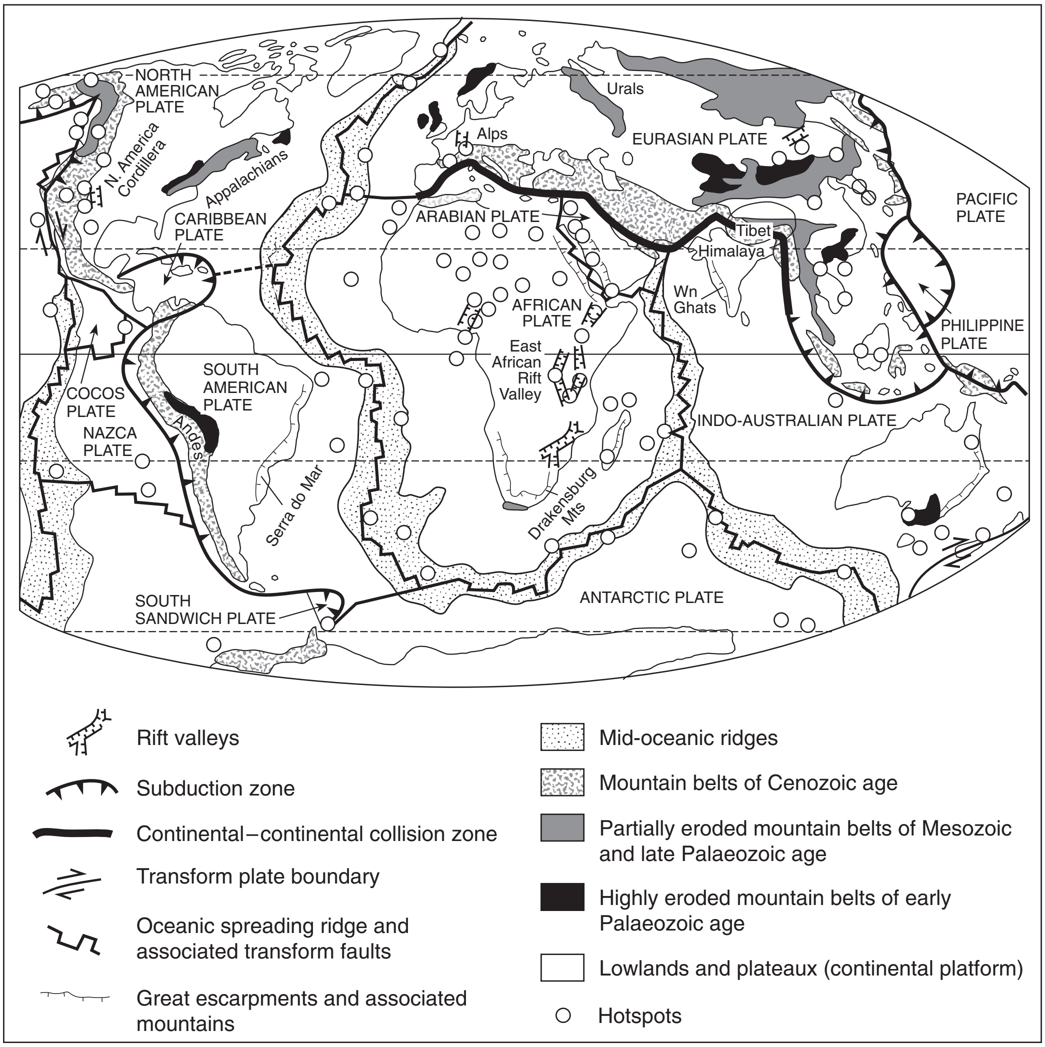

Figure 2.1 *The distribution of mountain systems showing their relationship to plate boundaries and tectonic settings*
Adapted from Uyeda (1978), Vogt (1981) and Summerfield (1991a).

was subsequently broken up with the opening of the Atlantic and is extensively covered by Mesozoic (~250 Ma to ~65 Ma) continental margins and the Atlantic Ocean. Nevertheless, its remains still constitute impressive mountain ranges.

The study of young active mountain systems provides knowledge and understanding of the dynamics of mountain building that may be used to understand contemporary and ancient systems, and can aid in effective management and hazard mitigation in mountainous regions. The aim of this chapter is to provide a framework for understanding the evolution of Cenozoic mountain systems that can be applied to help explain contemporary landscapes and the evolution of ancient and young orogens. Particular emphasis is placed on the Alpine–Himalayan–Tibetan orogen that constitutes part of the highest and greatest mountain mass on Earth and is hence one of the best natural laboratories to study the nature and dynamics of orogenic processes.

2 Geographic extent of global mountain belts

The association of young active mountains with plate boundaries reveals that major mountain systems occur in three main tectonic settings: continental–continental collision zones; subduction related settings (oceanic–oceanic and continental–oceanic collision zones); and oceanic spreading ridges. Other young mountains, however, are associated with transform plate boundaries, hotspots, rift systems and passive margins.

The longest mountain system is associated with the oceanic spreading ridges and extends for >40 000 km (Figure 2.1). Although these mountains may rise in elevation by >5 km from the ocean floors, they only occur above sea level where an oceanic spreading ridge astrides a hotspot. The Icelandic hotspot that is broadly coincident with the mid-Atlantic ridge and helps to form Iceland provides a contemporary example (Gudmundsson, 2000).

The largest mountain mass on Earth, however, is the Alpine–Himalayan–Tibetan system. This stretches from the Betic Mountains in Southern Spain through the European Alps, the Turkish–Iranian Plateau, the Zagros Mountains, the Himalaya, the Tibetan Plateau, to the Sumatra arc of Indonesia and is some 7000 km long and exceeds 2000 km at its widest part (Figure 2.1). Mountain ranges such as the Tien Shan and Gobi Altai Mountains are also part of this orogen. These mountains are associated with the collision of the African and Indian continental lithospheric plates with the Eurasian continental lithospheric plate.

The Circum-Pacific oceanic–oceanic and continental–oceanic collision zones constitute the next major mountain systems of note. These include the Antarctic Peninsula, Andes, Western Cordillera of North America, and the volcanic island arcs of the Aleutians through to Japan and the Philippines and on to New Guinea (Figure 2.1).

Mountain systems that are associated with other tectonic settings and include transform plate boundaries, passive margins and hotspots are not really of continental/global scale but are impressive topographic features (Figure 2.1). These include the Alps of New Zealand, which provide one of the best examples of a mountain system associated with a transform plate boundary. This is the result of the relative motion between the Antarctic, Indian–Australian and Pacific plates (Tippett and Hovius, 2000; Williams, this volume). The Transverse Ranges of Southern California within the San Andreas–Gulf of California transform system provide another example of a mountain system within a transform plate boundary (Cox *et al*., 2003). These essentially form within the double bend of the San Andreas fault system and they rise from a few hundred metres to 3500 m above sea level (asl) within little more than 10 km.

The Western Ghats of India and Drakensberg Mountains of South Africa are impressive examples of mountain ranges that have formed along passive margins (cf. Ollier, this volume). These are thought to be the result of uplift due to denudational unloading and isostatic flexuring as the adjacent plateau regions are eroded along their margins (Gilchrist and Summerfield, 1990, 1994; Summerfield, 1991a, b; Brown *et al*., 2000; Gunnell and Fleitout, 2000).

Mountains produced by hotspots are a consequence of regional warping and associated volcanism and rifting. The Grand Tetons in Wyoming provide a spectacular example of uplift along a rifted margin associated with a hotspot, in this case related to the Yellowstone hotspot (Love and Reed, 1971; Pierce and Morgan, 1992). The Hawaiian Islands–Emperor Seamount chain provide an example of volcanic mountains that have grown over the Hawaiian hotspot as the Pacific plate has moved progressively northwestwards and then westwards over time. However, such mountains subside as they are tectonically transported away from the hotspot and as their mass increases and causes isostatic subsidence (Watts and ten Brink, 1989).

3 Characteristics of Cenozoic mountain belts

The greatest mountain systems traverse many climatic belts. As a consequence they include along their length nearly every environmental and geomorphic setting. For example, they may include tropical rainforest, deciduous forest, alpine meadows, tundra, desert and glacial environments (Troll, 1973a, b). Since most Cenozoic mountains exceed 5000 m asl, they are extensively glacierized. They commonly have a precipitation gradient across their ranges and rainshadows on their leeward slopes. The steep slopes and glacierized catchments result in high river discharges and extensive landsliding.

The geomorphic processes within these environments play a major role in shaping the landscapes. Furthermore, it is becoming increasingly apparent that denudation influences the tectonism in these regions by such processes as denudational unloading and basin subsidence resulting from the thick piles of sediments that are deposited in the forelands (Montgomery, 1994; Gilchrist *et al*., 1994; Shroder and Bishop, 2000; Bishop *et al*., 2002).

Dramatic climatic changes have taken place throughout the Cenozoic, and particularly throughout the Quaternary. This has caused major fluctuations in the magnitude and frequency of Earth surface processes in mountain regions. Moreover, the mountain uplift may have also contributed to climate change throughout the Cenozoic by affecting global atmospheric circulation, deflecting jetstreams, initiating and enhancing monsoons and altering biogeochemical cycles (Ruddiman and Kutzbach, 1989; Raymo and Ruddiman, 1992; Ruddiman, 1997, 1998; Ramstein *et al*., 1997). Such are the links and feedbacks between tectonism, climate, Earth surface processes and biology that research in the evolution of Cenozoic mountain systems is becoming increasingly multidisciplinary.

Despite the variety of tectonic and geomorphic settings for mountain systems, the two largest subaerial mountain systems, the Alpine–Himalayan–Tibetan and the Circum-Pacific systems, have a number of similarities in their evolution and geologic characteristics. In the mature stages of the orogen, the mountain system may be broadly divided into geologic and topographic belts. These are illustrated in Figure 2.2(A) and include:

1 an outer foredeep or foreland basin;
2 a foreland fold-and-thrust belt;
3 a crystalline core complex that includes: sedimentary rocks and their basement; volcanic and igneous rocks and associated sediments; metamorphosed ocean crust (ophiolites); gneissic terranes with abundant ultramafic bodies; and granitic batholiths;
4 rectilinear (high-angle) fault zones.

The Himalayan–Tibetan region illustrates this well. It exhibits all these belts, although they are developed to varying degrees along different transects of the orogen (Figure 2.2(B)–(D)).

Geologic observations of orogenic belts suggest that a sequence of events occurs as part of an orogenic cycle (Moores and Twiss, 1995). These events are summarized in Table 2.1. Dilek and Moores (1999) illustrate some of these similarities in their comparative study of the early Tertiary Western United States Cordillera and the modern Tibetan and Turkish–Iranian Plateau. They stressed that, as a consequence of an orogenic belt becoming overthickened, the mountains become the loci of lithospheric extension and experience tectonic collapse during their late-stage post-collisional evolution. It follows that the hinterland of major orogenic belts share a common taphrogenic (rifting) evolutionary path. This is related to rapid increase in the geothermal gradient and thus rapid isobaric heating, prograde high-temperature metamorphism, intrusion of post-tectonic granites and the extrusion of ignimbrites and associated minor extension. This phase is commonly followed by a further increase in the geothermal gradient, accelerated lithospheric extension and thinning with erosional denudation, superposition of high-temperature/low-pressure metamorphic assemblages, mantle partial melting

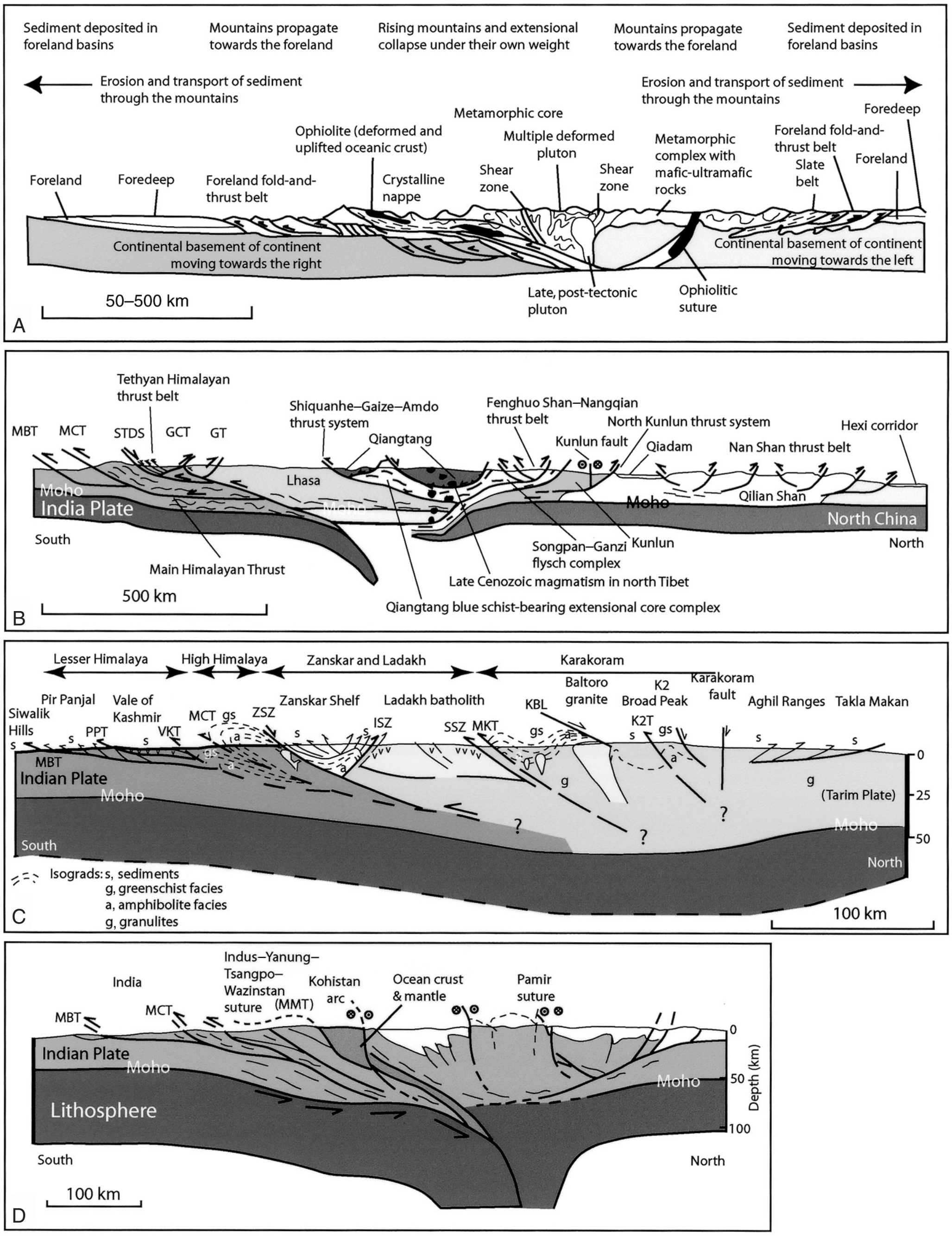

Figure 2.2 *Comparison of selected cross-sections across the Himalayan–Tibetan orogenic belt with a schematic cross-section across a model composite orogenic belt. (A) Model composite orogenic belt showing the major structures and tectonic components (adapted from Hatcher and Williams, 1986, and Moores and Twiss, 1995). Schematic sections across (B) the Himalaya, Tibet and Qilian Shan from Nepal to the Hexi Corridor (after Yin and Harrison, 2000); (C) the western Himalaya and central Karakoram (after Searle, 1991); and (D) the Himalaya, Kohistan and Pamir (adapted from Mattauer, 1986). Figure 2.5 shows the locations of sections (B), (C) and (D). GCT, Greater Counter Thrust; GT, Gangdese Thrust; ISZ, Indus Suture Zone; K2T, K2 Thrust; KBL, Karakoram Batholith Lineament; MBT, Main Boundary Thrust; MCT, Main Central Thrust; MKT, Main Karakoram Thrust; MMT, Main Mantle Thrust; PPT, Pir Panjal Thrust; STDS, South Tibet Detachment System; SSZ, Shyok Suture Zone; VKT, Vale of Kashmir Thrust; XF, Xianshuihe Fault; ZSZ, Zanskar Shear Zone. The Moho marks the boundary between the crust and the mantle*

Table 2.1 – Sequence of events in an orogenic cycle

1	Accumulation in separate areas of thick deposits of both shallow-water and deep-water marine sediments, the latter in association with intrusions or extrusions of mafic or intermediate magmatic rocks
2	Commencement of deformation in the foreland fold-and-thrust belt together with the emplacement of ophiolitic rocks and the subsequent isostatic rise of the ophiolite and the deformed sediments beneath it
3	Continued deformation in the fold-and-thrust belt – and metamorphism, deformation, and intrusion of granitic batholiths in the core zone – together with deposition of synorogenic sediments
4	Further isostatic rise of the orogenic region and the deposition and partial deformation of post-orogenic continental sediments in the outer foredeep
5	Block faulting, the development of fault-bounded basins, and the intrusion of scattered alkalic dykes and intrusive bodies

Source: Moores and Twiss (1995).

and mafic magmatism, and rapid subsidence and deposition of nonmarine sediments. This sequence of events and the similarity of tectonic structures for the Tibetan Plateau and Himalaya, Turkish–Iranian Plateau, and Western US Cordillera and Great Basin are summarized in Table 2.2 and Figure 2.3. In Figure 2.3(C) it should be noted that the North American craton is underplating the Sevier thrust belt and the overall morphology and tectonics of the high plateau and the Great Basin are analogous to the Tibetan Plateau and Turkish–Iranian Plateau. Furthermore, the Great Basin, Himalayan–Tibetan and Turkish–Iranian plateaux all adjoin a suture zone (union of lithospheric scale units), where continental apposition occurred and where major shortening and imbrication took place resulting in crustal overthickening and surface uplift.

Clearly, these observations and sequence of events are somewhat simplistic and the evolution of each individual orogen varies spatially and temporally. This model, however, does provide a working framework to help understand the evolution of Cenozoic and ancient mountain systems. Some of these differences and the detailed evolution of several of the major mountain ranges will now be discussed in more detail.

4 Alpine–Himalayan–Tibetan orogenic belt

The Alpine–Himalayan–Tibetan orogenic belt incorporates the Betic Mountains, European Alps, Zagros, Himalaya, Trans-Himalaya, Tibetan Plateau and its ranges, Tien Shan and the Gobi Altai. Several major zones of continental–continental collision are evident along its length and these include: the Alps (African–European collision); the Turkish–Iranian Plateau (Arabian–Asian collision); and the Himalayan–Tibetan orogen (Indian–Asian collision) (Figure 2.1). These major zones of convergence, for most of the orogen, are shown in Figure 2.3(C). Until the beginning of the 1980s little attention had been given to the orogen outside of the Alps. This was mainly due to political and logistical problems. However, during the last two decades considerable efforts have been made to study the evolution of Tibet and its bordering mountains. Unfortunately, studies of the Turkish–Iranian Plateau are still few because of the difficulties of fieldwork in this politically sensitive part of the world.

Some of the first orogenic studies were undertaken in the European Alps and their influence still persists in modern geology (Hsu, 1995). For example, the concept of fold nappes (sheet-like units of deformed rock that have moved on a predominant horizontal surface as a result of thrust faulting, recumbent folding or both mechanisms) was first introduced in 1841 by an Alpine geologist, Escher

Table 2.2 – Nature and chronology of tectonic and magmatic events during the taphrogenic evolution of orogenic belts with comparisons from the Tibetan Plateau and Himalaya, Turkish–Iranian Plateau, and Western US Cordillera and Great Basin

TECTONIC EVENT	MAGMATISM	TIBETAN PLATEAU & HIMALAYA	TURKISH-IRANIAN PLATEAU	WESTERN US CORDILLERA & GREAT BASIN
Block-faulting & thick-skinned extension	Bimodal volcanism (alkaline basalts and peralkaline rhyolites); subcontinental mantle involvement in magmatism	E–W extension Basaltic volcanism (6–0 Ma) Calcalkaline volcanism	E–W extension Alkaline basaltic volcanism, basanite (5–0 Ma)	Block-uplift of the Sierra Nevada (6 Ma) Bimodal volcanism (17–0 Ma) Basin & Range extension: block-faulting, regional subsidence (17–0 Ma)
Thin-skinned extension, denudation, crustal exhumation; tectonic escape via lateral extrusion	K-rich, aluminous silicic to intermediate magmatism (crustal isotope ratios)	Peraluminous granites (15–10 Ma) Leucogranites (28–12 Ma) N–S shortening, E–W strike-slip faulting	N–S shortening: thrust and strike-slip faulting (12–0 Ma) High-K, high-Al rhyolite ignimbrites (8–6 Ma) Metamorphic core complex formation (Miocene)	Pre-Basin & Range extension 'Ignimbrite flare-up', rhyolitic to dacitic, andesitic eruptions; shallow-level granite intrusions (40–17 Ma) Metamorphic core complex formation (Late Eocene–Oligocene)
Collision, contraction, crustal thickening; ophiolite emplacement	Peraluminous granites (S-type); crustal anatexis	India-Eurasia collision (~40 Ma) Ophiolite emplacement (Late Cretaceous)	Arabia-Eurasia Collision (M. Miocene) Granitic intrusions Pontide-Anatolide Collision (Late Eocene) Ophiolite emplacement (85–75 Ma)	Two-mica granites (80–65 Ma) Strike-slip faulting (Late Mesozoic–Early Cenozoic) Sevier orogeny (110–90 Ma) Ophiolite emplacement (175–157 Ma)

After Dilek and Moores (1999). Reproduced with the permission of the Geographical Society of London.

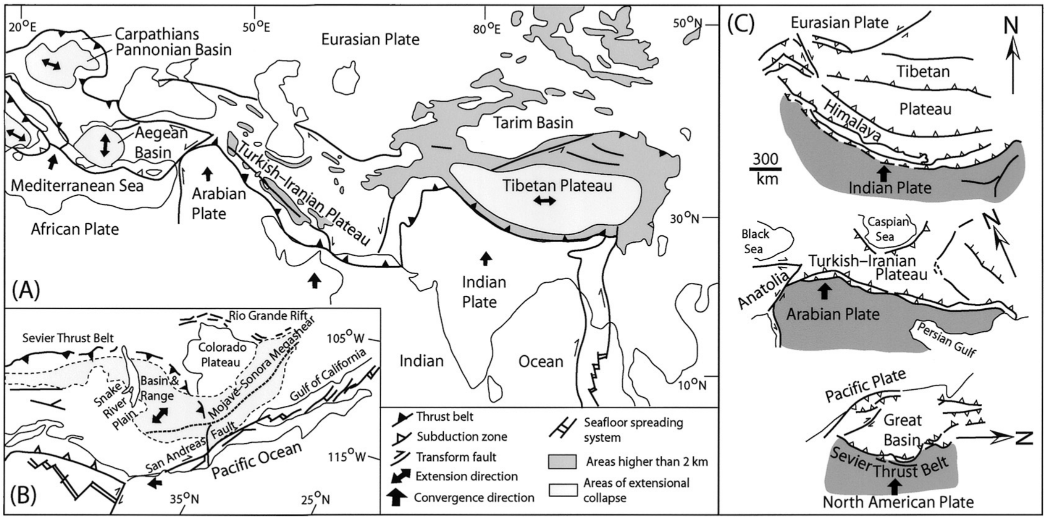

Figure 2.3 *Simplified tectonic maps of the (A) Alpine–Himalayan–Tibetan orogenic belt and (B) the Western US Cordillera showing areas of high elevation (>2000 m asl), extensional orogenic collapse, and plate convergence. (C) Simplified tectonic maps of the Himalaya–Tibet, Turkish–Iranian Plateau, and the pre-Basin and Range Western US Cordillera at the same scale. The plate boundaries, geometry of the collision zones, and the direction of relative plate motion are shown. Large arrows show the direction of relative plate motion*
Adapted from Dilek and Moores (1999).

van der Linth (Ryan, 2000). Despite the Alps being the most studied of all orogenic belts, its history has still to be fully understood because of its complex evolution involving a combination of subduction of Mesozoic oceanic crust, ophiolite emplacement, back-arc spreading, volcanism, metamorphism, thrusting and nappe emplacement, denudation and foreland basin sedimentation.

The Alpine sector of the Alpine–Himalayan orogenic belt is extensive, stretching from Gibraltar to Turkey, and includes the Betic Mountains, European Alps, Dinarides, Hellenides and Carpathians, while the Turkish–Iranian sector includes the Turkish–Iranian and Zagros Mountains (Figures 2.3 and 2.4(A)). The Alpine–Iranian belt developed on late Palaeozoic Hercynian (~345–225 Ma) and late Proterozoic–early Palaeozoic Pan-African (~800–500 Ma) orogenic belts as the continental plates of Africa and Arabia advanced into the Eurasian continental plate. The movement of Africa and Arabia into Eurasia is the consequence of the opening of the Atlantic and Indian Oceans. The convergence history is therefore complex and this has resulted in an orogen that varies considerably along its length. It has also resulted in abrupt curves and large changes in the strike of fold-and-thrust belts along its length. Bends of 90° to 180°, for example, characterize the Gibraltar region, the Alps, the Carpathians and the Balkanides. These bends, together with the complex fold-and-thrust vergences, suggest that considerable rotation and/or strike-slip deformation must have taken place. Furthermore, as illustrated in Figure 2.4(B), the orogen is more complex than the simple bilateral model shown in Figure 2.2(A). This section through the Swiss Alps shows two outward-directed thrust sequences on either side of a metamorphic core, associated with an apparent offset of the Moho (the Mohorovičić Discontinuity, which marks the boundary between the crust and mantle). In comparison, the orogen is more symmetrical in the Dinarides and the Carpathians where thrusts verge in opposite directions away from the volcanic rich Pannonian Basin (Figure 2.4(A)). Similarly in Turkey, the Tauride and Pontide thrust complexes bound either side of a central core of deformed and metamorphosed rock and younger volcanic rock that underlie the central Anatolian Plateau (Moores and Twiss, 1995).

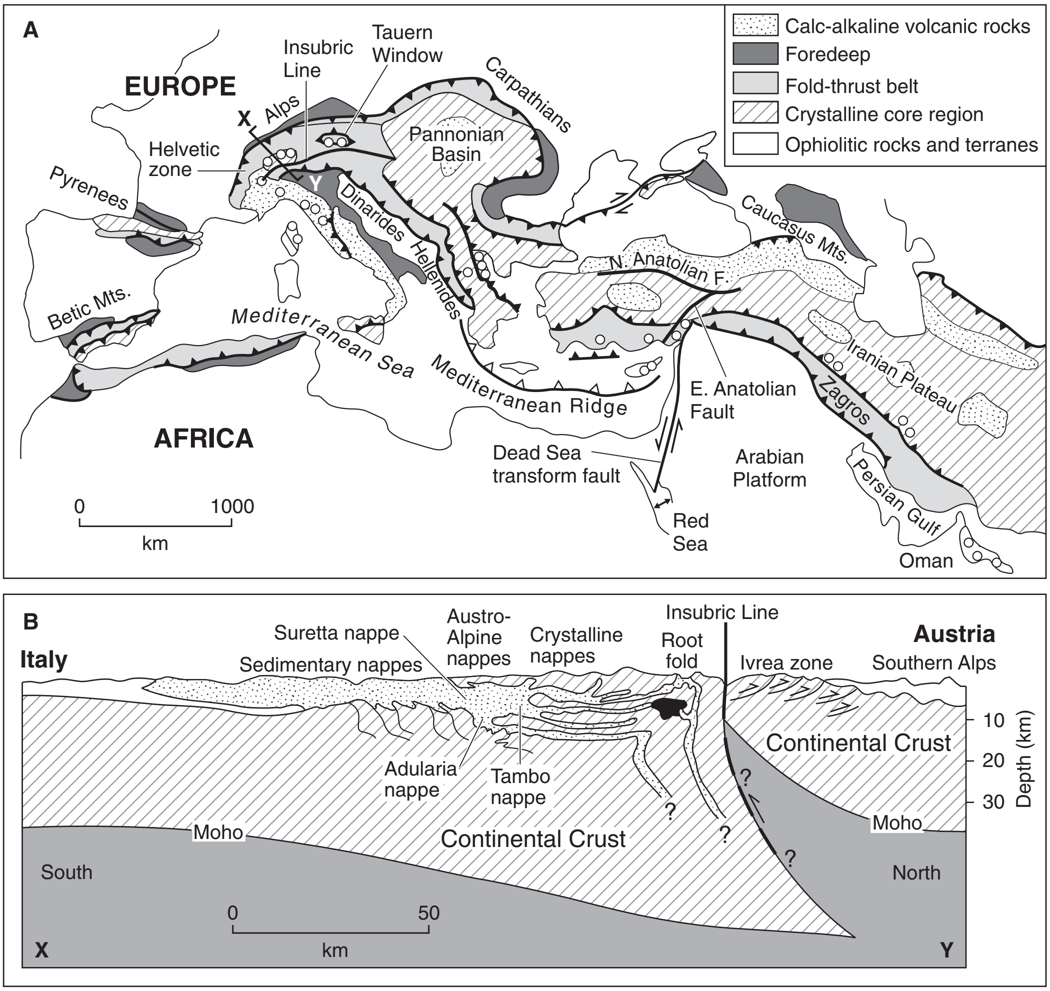

Figure 2.4 *Characteristics of the Alpine–Mediterranean sector of the Alpine–Himalayan orogenic belt. (A) Simplified geologic map showing the main structural features (adapted from Dewey* et al.*, 1973, and Moores and Twiss, 1995). (B) Cross-section through the Swiss Alps showing recumbent nappes and root fold in the crystalline core zone of the Alps (after Laubscher, 1982)*

No one model explains the tectonic evolution of the whole of the Alpine–Iranian sector. Nevertheless, much of the alpine sector can be explained by developing a model that involves the formation and deformation of island arcs and associated basins, and the collision of a microcontinent (Penninic) with the Apulia (eastern Italy, the Ionian Sea, Slovenia, Croatia, Bosnia, Albania, Montenegro, Greece and western Turkey), and ultimately Europe (Roeder, 1977). Simplified, the Alpine sector really began to form in the middle Cretaceous (~120 Ma) with the subduction of the southern ocean basin beneath an island arc that was separated from the passive margin of the Apulian terrane by a marginal basin. This was followed (~ 110 Ma) by the collision of the Penninic microcontinent and deformation of the overriding island arc and marginal basin. During the late Cretaceous (~90 Ma), the Apulian continental margin overrode the marginal basin intensifying the collision zone. Following this, the northern basin closed as it was subducted under an arc separated from the rifted passive margin (Helvetic miogeocline) by a back-arc basin. The southern continental mass collided and overrode the northern continental mass deforming the arc, back-arc basin and Helvetic miogeocline during the early Miocene (~20 Ma). Since the late Neogene (5–0 Ma) there has been continued convergence and shortening resulting in nappe emplacement and backfolding (Roeder, 1977; Moores and Twiss, 1995).

Although the Himalayan–Tibetan orogen is commonly considered to be one of the youngest mountain belts, its history spans far beyond the beginning of the Cenozoic. Initially, throughout the early Palaeozoic, this involved the sequential accretion of microcontinents and island arcs onto the southern margin of Eurasia (Hsu *et al*., 1995; Sengor and Natal'in, 1996). This was followed by the collision of the Indian continental lithospheric plate with the Eurasia continental lithospheric plate between 50 and 70 Ma (Yin and Harrison, 2000). During the past 40–50 Ma the Indian plate has been moving at a nearly constant rate of ~50 mm a^{-1} northward with respect to stable Eurasia, resulting in between 1400 and 2000 km of crustal shortening (Molnar and Tapponnier, 1975; Patriat and Achache, 1984; DeMets *et al*., 1994). Ultimately, this led to the formation of the present Tibetan Plateau and the adjacent mountains. The collision of India into Asia helped to rejuvenate the Tien Shan orogen and has affected regions as far north as the Gobi Altai Mountains and Baikal rift, and may have played a role in the opening of the South China Sea (Molnar and Tapponnier, 1975, 1978; Tapponier *et al*., 1986; Hendix *et al*., 1994; Abdrakhmatov *et al*., 1996; Cunningham *et al*., 1996).

The region is, seismically, one of the most active in the world (Holt *et al*., 1995; Chen and Kao, 1996; Chen *et al*., 1999). The partitioning of the post-collisional crustal shortening is complex and is essentially divided between crustal thickening and lateral extrusion along strike-slip fault systems (Avouac and Tapponier, 1993; Houseman and England, 1996). Estimating the post-collisional shortening is difficult because of the uncertainty associated with estimating the initial crustal thickness before the Indian–Asian collision and because the shortening is distributed beyond the Himalayan–Tibetan region, with a substantial amount occurring in the Tien Shan (Murphy *et al*., 1997). Yin and Harrison (2000) suggest that the shortening since the Indian–Asian collision is distributed as follows: >360 km across the Himalaya, >60 km across the Gangdese thrust system, ~250 km along the Shiquanhe–Gaize–Amdo thrust system, >60–80 km across the Fenghuo Shan–Nangqian fold-and-thrust belt, ~270 km across the Qimen Tagh–North Kunlun thrust system, and ~360 km across the Nan Shan thrust belt. Furthermore, they suggest that the shortening is expressed in two modes at the surface: (a) discrete thrust belts with relatively narrow zones of contraction or regional décollement (a detachment structure resulting from deformation), and (b) distributed shortening over a wide region involving basement rocks.

A compilation of the rates of shortening and strike-slip faulting on Holocene and late Pleistocene timescales is summarized in Figure 2.5. These data are based on measuring and dating offset landforms and displaced outcrops. The current rate of deformation is beginning to be quantified by Global Positioning System (GPS) measurements (King *et al*., 1997; Larson *et al*., 1999; Wang *et al*., 1999; Chen *et al*., 2000). These studies show relatively good agreement with the geologic data, yet they are somewhat limited by the short duration over which the measurements have been undertaken.

Numerous models have been constructed to help understand the geodynamics of the Indian–Asian collision and they involve numerical simulation of indentation of a viscous thin-sheet (England and McKenzie, 1982; Vilotte *et al*., 1982; England and Houseman, 1989; Ellis, 1996; Yang and Lui, 2000), analogue models of indentation of a plasticine plane (Tapponnier and Molnar, 1976; Tapponnier *et al*., 1986; Peltzer and Tapponnier, 1988) and three-dimensional (3-D) finite element modelling (Lui *et al*., 2000). Such modelling studies add to the knowledge and understanding of the deep structure of the Himalayan–Tibetan orogen and they complement the deep crustal research (Nelson *et al*., 1996; Owens and Zandt, 1997).

The timing of the Tibetan plateau uplift has been difficult to quantify because of the uncertainty in

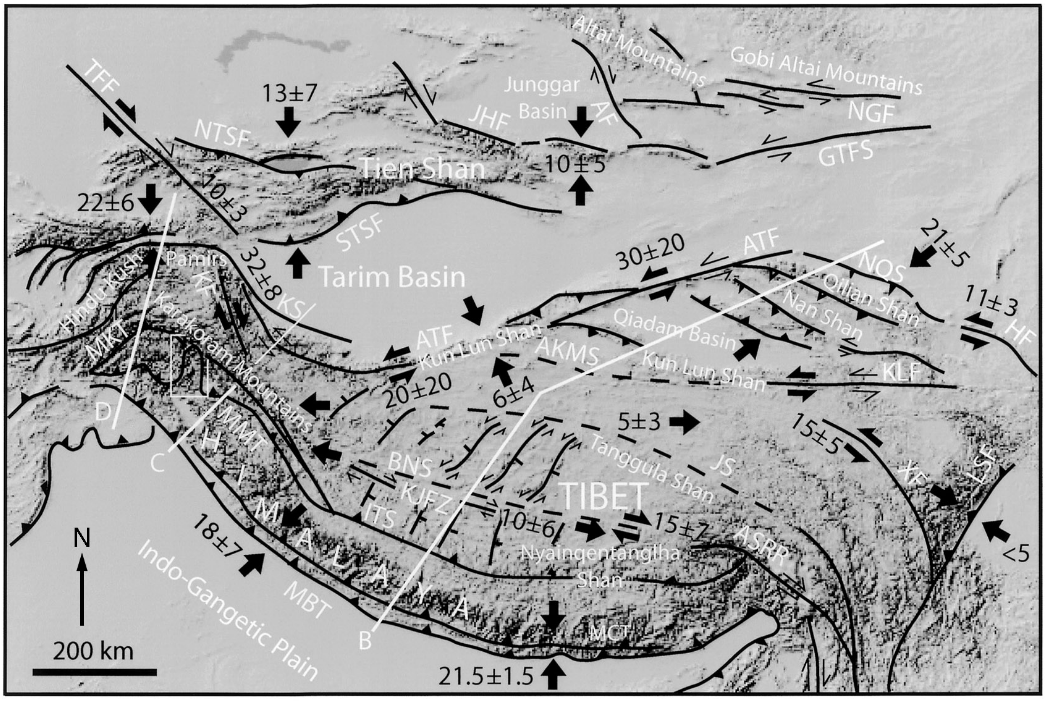

Figure 2.5 *Digital elevation model of Tibet and the bordering mountains showing the major faults and sutures. Estimates of late Quaternary strike-slip, convergence and extension rates are shown in millimetres per annum (after Larson* et al.*'s (1999) compilation of recent data). The sections B, C and D are shown in Figure 2.2. AF, Altai fault; AKMS, Ayimaqin–Kunlun–Mutztagh suture; ASRR, Ailao Shan-Red River shear zone; ATF, Altyn Tagh fault; BNS, Bangong Nujiang suture; GTFS, Gobi–Tien Shan fault system; HF, Haiyuan fault; ITS, Indus Tsangpo suture; JHF, Junggar Hegen fault; JS, Jinsha suture; KF, Karakoram fault; KJFZ, Karakoram Jiali fault zone; KLF, Kunlun fault; KS, Kudi suture; LSF, Longmen Shan fault; MBT, Main Boundary Thrust; MCT, Main Central Thrust; MKT, Main Karakoram Thrust (Shyok suture zone); MMT, Main Mantle Thrust; NGF, North Gobi fault; NQS, North Qilian suture; NTSF, North Tien Shan fault; STSF, South Tien Shan fault; TFF, Talus–Fergana fault; XF, Xianshuihe Fault*
Adapted from Searle (1991); Cunningham et al. *(1996); Chung* et al. *(1998); Yin* et al. *(1999); Yin and Harrison (2000); Blisniuk* et al. *(2001); Hurtado* et al. *(2001).*

determining palaeoaltitudes (cf. Gregory and Chase, 1992). Several uplift patterns have been proposed (Harrison *et al*., 1992, 1998), but recent geologic data suggest that the initiation and rates of uplift varied considerably across the orogen (Chung *et al*., 1998). Furthermore, Murphy *et al*. (1997) suggested that a significant portion of southern Tibet was elevated before the Indian–Asian collision and Chung *et al*. (1998) suggested that northeastern Tibet had uplifted by 40 Ma, while in western Tibet the uplift occurred at about 20 Ma. These observations are consistent with sedimentation records from the Ganges–Brahmaputra delta and the Bengal fan (Chung *et al.*, 1998). The uplift history also helps to explain the nature of the strontium isotope evolution of the oceans and global cooling over the past 20 Ma (Chung *et al*., 1998).

By about 14 Ma, the Tibetan Plateau had become sufficiently thick that it began to extend gravitationally (Coleman and Hodges, 1995). Two types of extensional structures are apparent: the south Tibetan fault system, a family of east-striking shallow to moderate north-dipping normal faults exposed near the crest of the Himalaya from Bhutan to northwest India; and numerous north-trending rift systems that largely dictate the topographic pattern of the southern Tibetan Plateau (Armijo *et al*., 1986; Wu *et al*., 1998; Yin *et al*., 1999; Yin, 2000; Blisniuk *et al*., 2001; Hurtado *et al*., 2001). These structures are summarized on Figure 2.5 and the relationship to the evolution of the Himalayan–Tibetan orogen is reviewed in Table 2.2 and Figure 2.2.

The uplift and subsequent denudation of the Himalayan–Tibetan orogen resulted in a varied topography and geology. This is summarized in Figures 2.2 and 2.5. Several pervasive structures are present along the length of the Himalaya. These include: the Main Boundary Thrust that delimits the southern margin of the Himalaya; the Main Central Thrust that forms a major crustal suture zone within the Indian plate; and the Main Mantle Thrust (Indus Tsangpo Suture) that marks the main boundary between the Indian and Asian continental plates. Other major thrusts and sutures are present, but they are not so regionally pervasive; they include the K2 Thrust, Karakoram Batholith Lineament, Pir Panjal Thrust and the Vale of Kashmir Thrust. Several major sutures traverse Tibet and include the Bangong Nujiang, Jinsha and Ayimaqin–Kunlun–Mutztagh sutures, which started to form during the Palaeozoic. In addition, continental-scale strike-slip fault systems transverse Tibet and include the Karakoram, Altyn Tagh and Kunlun faults, and the Ailao Shan–Red River Shear Zone. These are considered to be important in allowing the regional shortening to be accommodated as eastward lateral extrusion (Tapponnier and Molnar, 1976). For example, the total slip along the Altyn Tagh fault during the Cenozoic probably exceeds 600 km (Yin and Harrison, 2000) and along the Karakoram fault it is $>$100 km (Searle and Owen, 1999). The Altyn Tagh and Karakoram faults act as major transfer faults linking major thrust belts and extensional systems, respectively (Figure 2.5).

The Trans-Himalayan Batholith is an important component of the Himalayan orogen. It is discontinuous along the entire length of the Trans-Himalaya, some 2500 km. Along the eastern stretch it occurs north of the Indus–Tsangpo suture and it was emplaced into an Andean-type margin during the mid-Cretaceous and in the Palaeocene–lower Eocene (England and Searle, 1986; Debon *et al*., 1986). In the west, in northern India and Pakistan, it forms the Kohistan–Ladakh arc. This was an island arc that grew on the northern side of the Neo-Tethys Ocean that separated India from Eurasia during the mid-Cretaceous. The arc collided with the Karakoram plate at between 102 and 85 Ma to become the leading edge of an active continental margin under which the Neo-Tethys was subducted (Petterson and Windley, 1985; Coward *et al*., 1987; Reuber, 1989) (Figures 2.2(C) and 2.2(D)). This arc was intruded by an Andean-type granodiorite batholith between 78 and 75 Ma, and 48 and 45 Ma (Sullivan *et al*., 1993). The Indian plate eventually collided with the arc during the earliest Eocene and the continuous underthrusting of the Indian plate below the arc led to crustal thickening and melting and the intrusion of leucogranites at $\sim$30 Ma and subsequent deformation (Petterson and Windley, 1985).

The occurrence of syn-collisional igneous activity is an important characteristic of the Himalayan–Tibetan orogen (Figure 2.2(B)–(D); Table 2.2). Yin and Harrison (2000) listed five different mechanisms that may have been responsible for the generation of syn-collisional igneous activity. These are: (i) an early crustal thickening followed by slip along a shallow dipping décollement (Himalayan leucogranites); (ii) slab break-off during the early stage of the Indian–Asian collision (Linzizong volcanic sequence in southern Tibet); (iii) continental subduction in southern and central Tibet, which generated calcalkaline magmatism; (iv) formation of releasing bends and pull-apart structures that serve both as a possible mechanism to generate decompressional melting and as conduits to trap melts (Pulu basalts and other late Neogene–Quaternary volcanic flows along the Altyn Tagh and the Kunlun faults); (v) viscous dissipation in the upper mantle and subduction of Tethyan flysch complexes to mantle depths may be the fundamental cause of widespread and protracted partial melting in the Himalayan–Tibetan orogen in the Cenozoic.

The presence of calcalkaline type volcanism in southern and central Tibet suggests that some portion of the continental crusts from both the north and south must have been subducted into the mantle beneath Tibet (Yin and Harrison, 2000).

The role of denudation in shaping the Himalayan–Tibetan region is a subject of intense debate. Molnar and England (1990), for example, hypothesized that Cenozoic climatic change would have increased glaciation throughout the Himalaya and this, and its associated processes, would have increased erosion creating deeply incised valleys. They argued that high isolated mountain peaks would have been isostatically uplifted because of the denudation unloading caused by the deep valley incision. This helps increase the maximum elevation of the mountains. Others argue that the geometry of the valleys and the erosion rates are not significant to allow such uplift to occur (Harbor and Warburton, 1992; Whittington, 1996; Whipple and Tucker, 1999).

Zeitler *et al*. (2001) proposed an interesting model relating erosion, geomorphology and metamorphism in the Nanga Parbat Himalaya in northern Pakistan. Nanga Parbat is the ninth highest mountain in the world and is essentially defined by the Main Mantle Thrust that forms a syntaxis around Nanga Parbat and Haramosh massifs (Figure 2.6(A)). The core of the Nanga Parbat massif is characterized by very young (<3 Ma) granites, low-P cordierite-bearing granulites, low seismic velocities, resistive lower crust and shallow microearthquakes implying shallow brittle-ductile transition bowed upwards by ~ 3 km. Incision rates for the Indus River in this region are in the order of 2–12 mm a^{-1} (Burbank *et al*., 1996) and tributary valley incision rates around Nanga Parbat are 22 ± 11 mm a^{-1} (Shroder and Bishop, 2000). Zeitler *et al*. (2001) proposed that the incision that produced the deep river gorge of the Indus helps weaken the crust in this region. This, in turn, encourages failure and helps draw in advective flow toward the topographic gap (Figure 2.6(B)). This builds elevation and, together with the incising river, builds relief and leads to high erosion rates. The result is a steepened thermal gradient, which raises the brittle-ductile transition, and further weakens the crust. Deep and mid-crustal material can then experience decompression melting and low-P–high-T metamorphism as it is moved rapidly to the surface. They called this process a 'tectonic aneurysm' and they believe that this is an important orogenic process in continental–continental collision zones.

The study of these continental–continental collision zones provides an insight into the evolution of the continents and helps in understanding and explaining the nature and distribution of ancient mountain systems. It is necessary, however, to examine active oceanic–oceanic and oceanic–continental

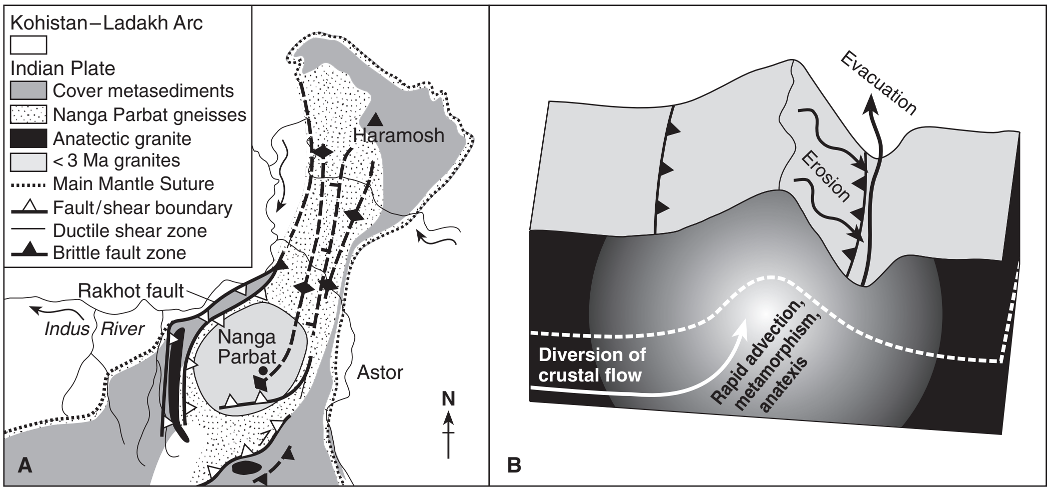

Figure 2.6 *The geology of Nanga Parbat massif, northern Pakistan, illustrating the relationship between erosion, crustal processes and uplift. (A) Geologic sketch map of the Nanga Parbat massif (after Schneider* et al., *1999, and Zeitler* et al., *2001). (B) Schematic representation illustrating the dynamics of a tectonic aneurysm, shown at a mature stage (see text for explanation) (after Zeitler* et al., *2001)*

collision zones to fully understand the early evolution of continental–continental collision zones. The Circum-Pacific orogenic belt provides such an opportunity and, ultimately, it may itself become a continental–continental collision zone in the distant future.

5 Circum-Pacific orogenic belt

The Circum-Pacific orogenic belt can be broadly divided into eastern and western sectors (Figure 2.1). The western sector of the Circum-Pacific orogenic belt is the result of convergence of oceanic plates including the Pacific, Philippine and Indian–Australian plates, and the eastern margin of the Eurasian plate (Figure 2.1). This sector, however, is discontinuous and includes volcanic island arcs and arc-collision zones. The associated mountains are not very geographically extensive, but nevertheless are impressive in terms of their relative relief and rates of erosion.

Taiwan, the Philippines, New Guinea and the Vanuatu arc in the southeast Pacific provide the best examples of arc–continental and arc–arc collisions. The convergence in this region is complex, with the interaction of the Pacific, Indian–Australian, Eurasian and Philippine plates, and two major trench–trench–trench triple junctions. Landforms include volcanic chains, fold-and-thrust belts and accretionary wedges. Taiwan provides one of the best examples of an area of rapid mountain uplift that is a consequence of arc–continental collision. The island rises to 3997 m asl and formed during the past 4.5 Ma as the Philippine Sea plate moved northwest into the Eurasian continental plate at a rate of $\sim$70 km Ma^{-1} (Seno, 1977; Angelier *et al*., 1986; Lee and Wang, 1987; Figure 2.7). Intense internal deformation and metamorphism has resulted in tectonic uplift rates of between 1 and 10 mm a^{-1} (Lin, 1991; Wang and Burnett, 1991). This uplift, together with rates of denudation of between 1 and 5 mm a^{-1} (Li, 1976) that are a consequence of the extreme monsoonal climate with its frequent tropical cyclones, has resulted in one of the youngest and most dynamic landscapes on Earth.

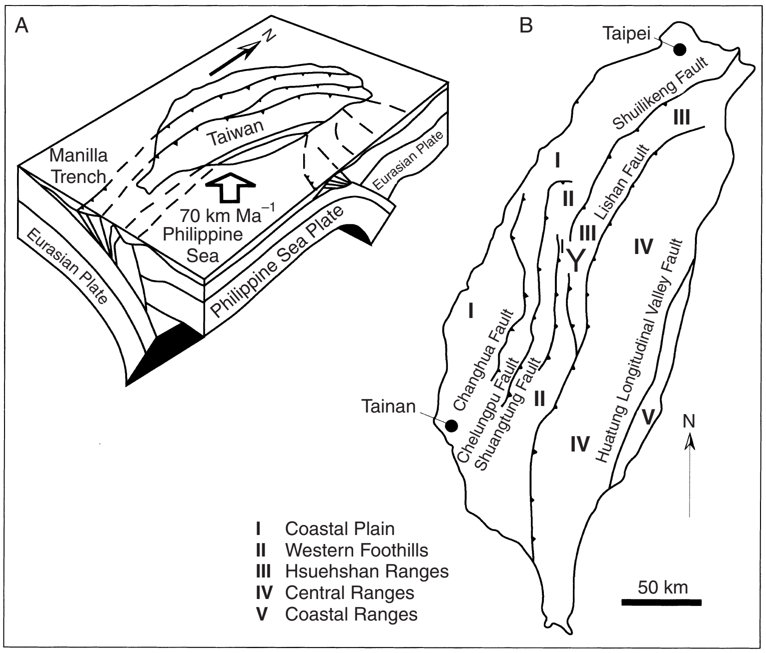

Figure 2.7 *The geologic setting of Taiwan and its associated mountain ranges. (A) Schematic plate tectonic setting (after Lin, 2000). (B) Major faults, and geologic and geomorphic units (after Chang, 2000)*

The Andes chain and North American Cordillera are the two greatest mountain ranges in the Circum-Pacific orogenic belt and stretch almost continuously for >20000 km. These constitute the eastern sector of the Circum-Pacific orogenic belt. Their evolution is essentially the consequence of the convergence of the oceanic and continental plates. Today this includes the collision of the Pacific, Juan Fuca, Cocos and Nazca oceanic plates with the North and South American continental plates (Figure 2.1). Presently, the margin is consumed beneath Alaska, the US Pacific Northwest and southwestern Canada, Central and South America, the Scotia Arc and the Antarctica Peninsula. Transform margins are present, connecting the trenches of Alaska and the Pacific Northwest and connecting the Mendocino triple junction to the Gulf of California, which comprises the San Andreas fault system (Moores and Twiss, 1995). The mountains along this sector of the Circum-Pacific orogenic belt have a long and complex history beginning in the late Precambrian. Most of the mountain building that produced the present landscapes, however, has occurred during the last 200 Ma (Figures 2.1 and 2.8). Structures verge towards the forelands on the eastern and western sides of the mountain belts, but there is a strong asymmetry within the orogens (Figure 2.8).

The Andean chain has been a site of continental accretion, crustal growth, and both compressional and extensional deformation throughout the Phanerozoic. Palaeozoic subduction and accretion resulted in the amalgamation of various terrains, associated with regional compression events (Ramos, 1988). Since the Triassic (~225 Ma) the southern Andes have formed a classic continental-type subduction margin and with no further terrain accretion. The northern Andes are more complex, influenced by Caribbean tectonics and the relative motion of the North and South America plates. This resulted in the accretion of island-arcs during the latest Mesozoic and early Tertiary. During the Jurassic and Cretaceous there was extensive rifting in fore-arc and back-arc basins, and magmatic activity along the length of the Andes that included the emplacement of massive granite batholiths (McCourt *et al*., 1984; Jaillard *et al*., 1990; Kay *et al*., 1991). Increased plate convergence occurred during the early Cenozoic and middle to late Cenozoic resulting in major regional deformation (Allmendinger *et al*., 1983; Jordan *et al*., 1983). During this time the eastern Andes flexed downwards in response to deformation and crustal loading. This resulted in a series of Cenozoic foreland basins that contain thick (≤5 km) sequences of terrestrial sediments. This general pattern of events is similar throughout the Andes, but, as illustrated in Table 2.3, the timing of orogenic events is diachronous along the mountain belt.

Like the Andes, the North American Cordillera has a complex history of continental accretion, crustal growth, and both compressional and extensional deformation. In addition, however, the southern stretch has also experienced the development of a continental transform plate boundary. This formed during the latter part of the Cenozoic, probably as a consequence of the subduction of the Pacific–Farallon ridge-transform system under North America (Atwater and Molnar, 1973; Atwater, 1989) (Figure 2.8). Several belts of deformation of different ages are present throughout the orogen. Palaeozoic deep-water rocks of the so-called 'eugeocline' were deformed by the Antler and Sonoma orogenies during the Devonian–Mississippian and Permo-Triassic, respectively (Speed *et al*., 1988). A phase of major deformation during the Sevier orogeny in the late Jurassic to late Cretaceous produced an extensive fold-and-thrust belt that extends from southeast California to Canada (Allmendinger and Jordan, 1981) (Figures 2.3 and 2.8). A complex hinterland of thick Palaeozoic shallow-water rocks of the 'miogeosyncline' is present east of this belt. These are involved in major Mesozoic nappes, Tertiary low-angled denudational faulting and metamorphic core complexes of Mesozoic and Tertiary age (Dilek and Moores, 1999). The easternmost segment of the North American Cordillera was deformed during the Cretaceous–Tertiary Laramide orogeny. This involves Precambrian crystalline crust and Palaeozoic–Mesozoic platform sedimentary rocks (Hamilton, 1988).

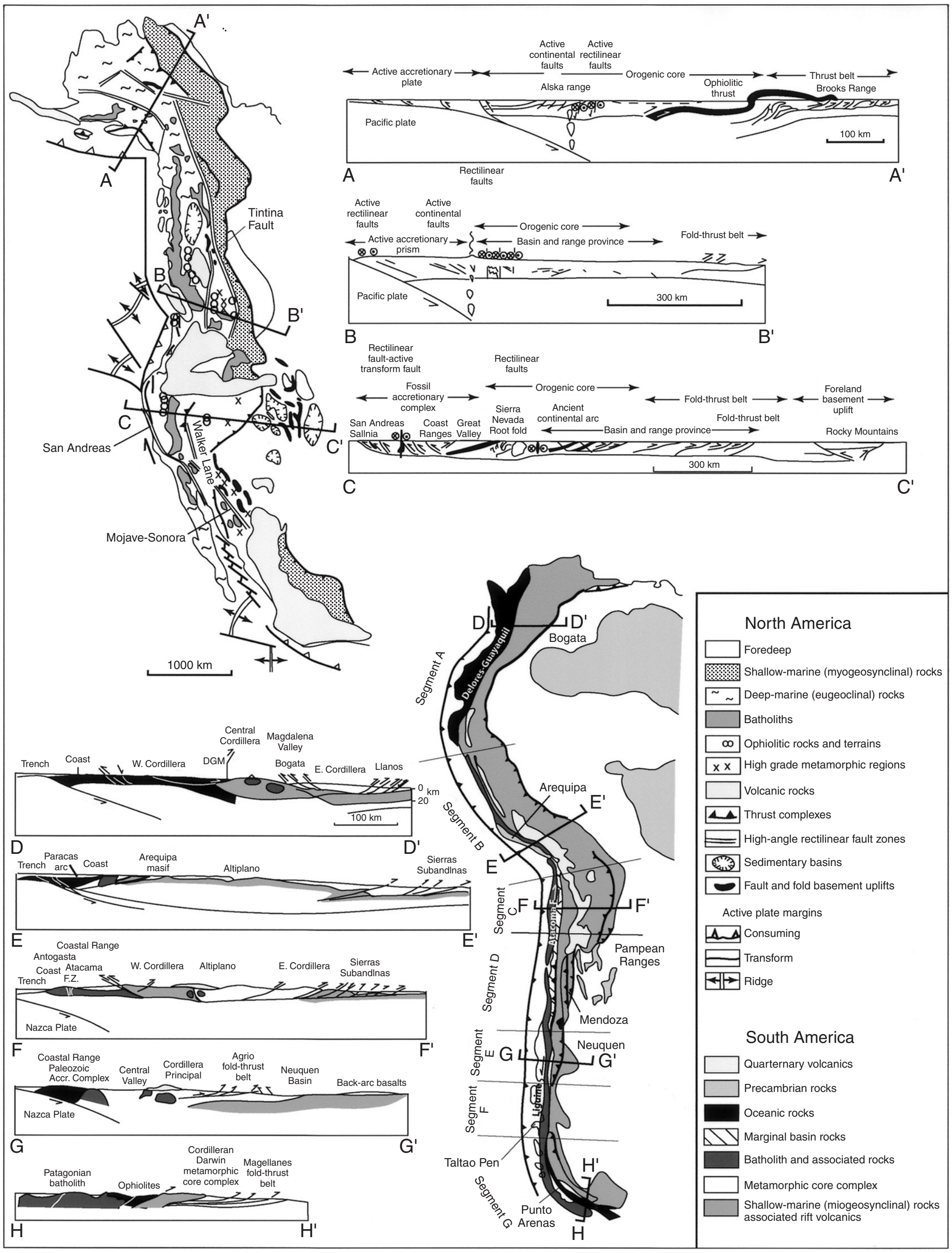

Figure 2.8 *Geologic characteristics of the North American Cordillera and Andes showing the major tectonic features. The Andes are divided into seven segments (A to G) and their geologic history is summarized in Table 2.3*
After King (1977), Megard (1989), Mpodozis and Ramos (1989) and Moores and Twiss (1995), and the geologic cross-sections are adapted from Moores and Twiss (1995), after Maxwell (1974), Roeder and Mull (1978), Csejtey et al. (1982), Potter et al. *(1986), Allmendinger* et al. *(1987), Roeder (1988), Mpodozis and Ramos (1989) and Vicente (1989).*

Table 2.3 – Time–space diagram showing the principal tectonic events along the length of the Andes

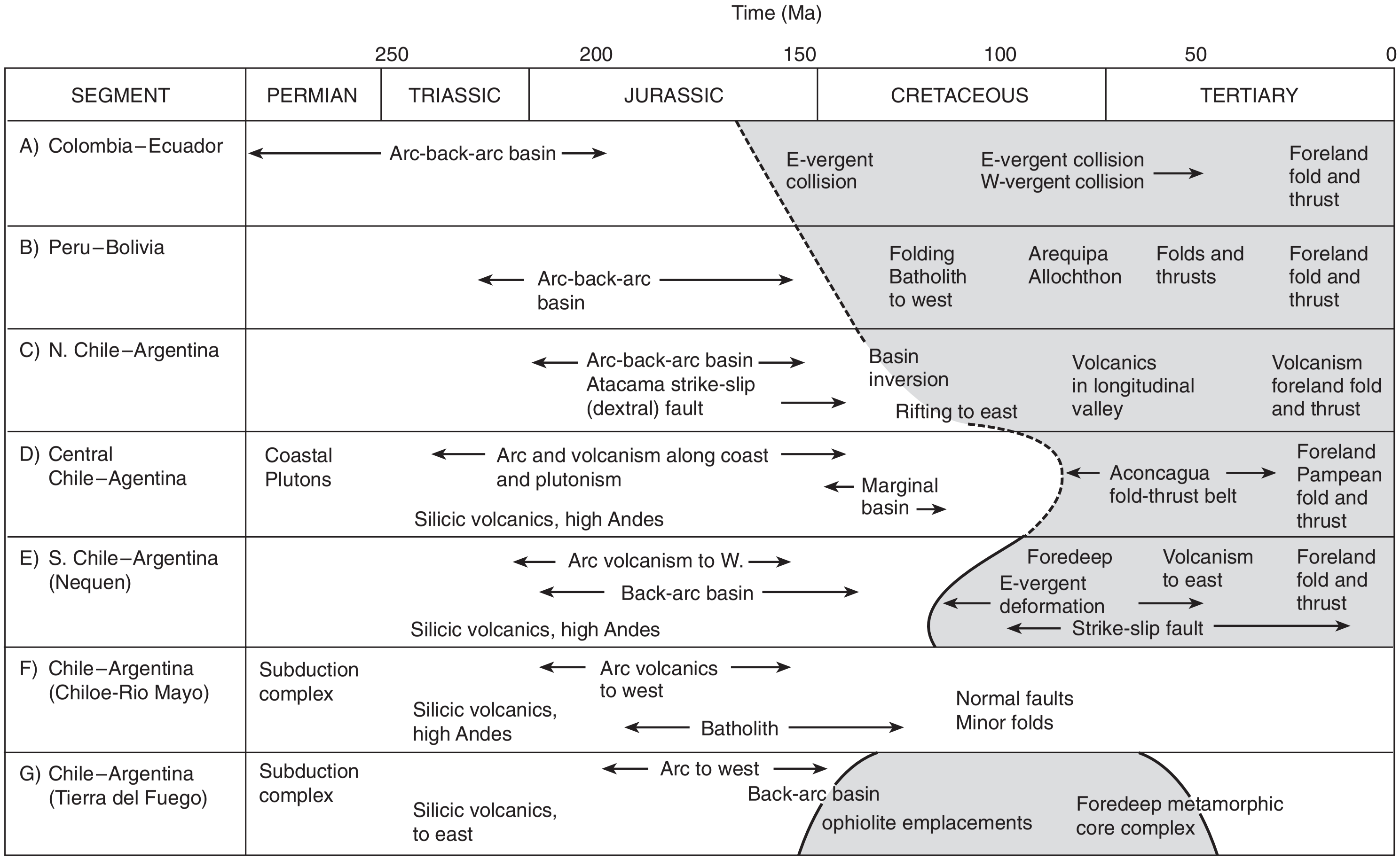

Notes: The heavy dashed line indicates the onset of the main Andean deformation. The location of each segment is shown in Figure 2.8.

After Moores and Twiss (1995).

The prolonged Mesozoic orogeny produced a north-trending crustal high that had a maximum thickness of about 60 km and an elevation of >3 km (Wolfe *et al*., 1997). By the mid-Tertiary, this highland region had begun to undergo orogenic extension resulting in the exhumation of metamorphic cores and widespread calcalkaline volcanism. The early stage of orogenic collapse was followed by the Basin and Range extension at between 18 and 16 Ma and associated volcanism (Coney, 1987). This ultimately produced the Great Basin with a mean elevation of ~1.5 km asl and a crustal thickness of ~30 km (Thompson and Burke, 1974; Wolfe *et al*., 1997). The succession of events that is important in producing the present orogen is summarized in Table 2.2 and discussed above in comparison with the Tibetan Plateau and the Turkish–Iranian Plateau.

The mountains of the Circum-Pacific orogenic belt help illustrate the variety of tectonic settings that can produce substantial relief along different types of convergent and transform plate boundaries. Furthermore, they provide valuable models for understanding the orogenic evolution of orogens that ultimately become continental–continental collision zones such as the Alpine–Himalayan–Tibetan orogen.

6 Ocean ridges

As a type of global mountain system, oceanic ridges are commonly neglected. This is probably because they are the least well studied owing to their inaccessibility. Ocean ridges occur in mid-ocean settings associated with divergent oceanic plates and back-arc spreading centres behind volcanic arcs of subduction zones. Mid-ocean ridges are between 1000 and 4000 km wide, they rise 2–3 km above the surrounding ocean floors and their crests have an average depth of 2500 m below sea level (Nicholas, 1995) (Figure 2.1). Back-arc spreading centres are considerably smaller than the mid-oceanic ridges and therefore little attention is given to them in this section.

Oceanic ridges are elevated because they consist of rock that is hotter and less dense than the adjacent oceanic crust. Furthermore, hot mantle material rises beneath the ridges to fill the gap created by the spreading plates and this helps to increase their elevation. As the mantle rises it decompresses and undergoes partial melting at depths that can exceed 100 km and over a broad region of several hundred kilometres. Gabbros form within magma chambers, and magma may be intruded into dykes and may erupt at the ocean floor to form basaltic shield volcanoes and lava flows. All this contributes to form new oceanic crust. As time progresses the new oceanic crust moves away from the spreading centre, cools, contracts and subsides. The spreading rates vary from a few millimetres per annum in the Gulf of Aden to 10 mm a^{-1} in the North Atlantic near Iceland and 60 mm a^{-1} for the East Pacific Rise, although the rates may vary over the duration of the ocean ridge's history (Reading and Mitchell, 2000).

Ridges with slow spreading rates have a well-defined (1.5–3 km deep) symmetrical axial rift valley. In contrast, the fastest spreading ridges have subdued topography more reminiscent of Hawaiian volcanoes, with a small summit ridge or graben (Macdonald, 1982). Well-developed axial valleys may drop to depths below that of the surrounding ocean floor. Hydrothermal activity is associated with ridges producing extremely hot springs that may form columnar structures known as chimneys.

Ocean ridges are broken into segments by transverse fractures (transform faults) which displace the ridges by tens, or even hundreds, of kilometres (Figure 2.1). These transform faults are sub-vertical and may produce fault scarps that exceed 500 m in height (Collette, 1986). Complex stress patterns are associated with the transform faults and transpressional and transtensional zones are common. Such stresses help to produce landforms analogous to those seen along continental strike-slip faults and include pressure ridges, pull-apart basins and shutter ridges.

The coincidence of the Icelandic hotspot with the mid-Atlantic ridge, that helped produce Iceland, provides an opportunity to examine some of the geologic aspects of oceanic ridges above sea level. However, the evolution of the ocean ridge at this location clearly differs from true oceanic ridges. This is because, for much of its history, it evolved by the successive subaerial and subglacial eruptions and a considerable portion of its uplift history and rifting is related to the hotspot (Gudmundsson, 2000).

As a consequence of the spreading, oceanic ridges are geologically young. Even with the slowest spreading rates, the rocks that comprise them are rarely more than a few tens of millions of years old. Nevertheless, they are among some of the world's most impressive geomorphic and tectonic features.

7 Conclusions

The above descriptions of the global mountain systems help illustrate their complex history, structure and morphology. Strong contrasts exist between global mountain systems that develop along mid-oceanic ridges, continental–continental collision zones and oceanic–oceanic/continental convergence zones. Furthermore, there is considerable variability within a single mountain system along any one plate boundary setting. This is really well illustrated along the Circum-Pacific and Alpine–Himalayan–Tibetan orogenic systems. Despite this, global mountain systems share a number of similar characteristics, both in their evolutionary path and the resultant forms. These are summarized in Figure 2.2(A) and Tables 2.1 and 2.2.

The evolution of individual mountain ranges may be in excess of hundreds of millions of years. Moreover, most Cenozoic mountain belts began their evolution long before the onset of the Cenozoic. Most orogenic belts grow outwards from a central core and may be diachronous along their lengths. Furthermore, uplift is not simple. It may propagate through a mountain system as the orogen evolves. In addition, as mountains grow in height, the denudation increases as a consequence of steeper slopes, increased river power and more prevalent mass movement, and possibly as a result of glaciation. High denudation rates may, in turn, contribute to uplift as a result of denudational unloading. The transfer of sediment to foreland regions may also contribute to uplift because of crustal flexuring associated with basin subsidence.

The growth of mountain ranges may also affect local, regional and even global climatic conditions. This, in turn, affects the rates and magnitudes of Earth surface processes that help shape the evolving orogen. This complex interaction between tectonic processes, climate and geomorphology needs quantifying to fully understand the links and interactions, and hence the evolution of global mountain systems. Fortunately, new analytical and computational methods and techniques are beginning to be applied to help explore and examine orogenic systems. Furthermore, much can be learned by applying space–time substitutions and by comparing ancient and modern mountain belts using tectonic, geomorphic and palaeoclimatological techniques. This is useful in helping to provide a fuller picture of the evolution of mountain belts and an understanding of their dynamics. It is encouraging that the study of orogenesis is becoming increasingly multidisciplinary, allowing for a better understanding of ancient and modern mountain systems. Such knowledge is also essential for sustainable development and hazard mitigation in mountain regions, especially as these regions become more populated, exploited and utilized by the world's growing population (cf. Hewitt, this volume).

Acknowledgements

I would like to thank Phil Owens, Mike Searle and Brian Whalley for very useful and constructive comments on an earlier version of this chapter.

References

Abdrakhmatov, K.Ye., Aldazhanov, S.A., Hager, B.H., Hamburger, M.W., Herring, T.A., Kalabaev, K.B., Makarov, V.I., Molnar, P., Panasyuk, S.V., Prilepin, M.T., Reilinger, R.E., Sadybakasov, I.S., Souter, B.J., Trapeznikov, A., Tsurkov, V.Y. and Zubovich, A.V., 1996. Relatively recent construction of the Tian Shan inferred from GPS measurements of present-day crustal deformation rates. *Nature*, **384**: 450–53.

Allmendinger, R.W. and Jordan, T.E., 1981. Mesozoic evolution, hinterland of the Sevier orogenic belt. *Geology*, **9**: 308–13.

Allmendinger, R.W., Hauge, T.A., Hauser, E.C., Potter, C.J., Klemperer, S.L., Nelson, K.D., Knuepfer, P. and Oliver, J., 1987. Overview of the COCORP 40°N transect, western USA. *Geological Society of America Bulletin*, **98**: 364–72.

Allmendinger, R.W., Ramos, V.A., Jordan, T.E., Palma, M. and Isacks, B.L., 1983. Paleogeography and Andean structural geometry, northwest Argentina. *Tectonics*, **2**: 1–16.

Angelier, J., Barrier, E. and Chen, H.T., 1986. Plate collision and paleostress trajectories in a fold-thrust belt: the foothills of Taiwan. *Tectonophysics*, **125**: 161–78.

Armijo, R., Tapponnier, P., Mercier, J. and Han, T., 1986. Quaternary extension in southern Tibet: field observations and tectonic implications. *Journal of Geophysical Research*, **91**: 13803–72.

Atwater, T., 1989. Plate tectonic history of the northeast Pacific and western North America. In Winterer, E.L., Hussong, D.M. and Decker, R.W. (eds), *The geology of North America*. Boulder, CO: Geological Society of America, volume N, 21–72.

Atwater, T. and Molnar, P., 1973. Relative motion of the Pacific and North American plates deduced from seafloor spreading in the Atlantic, Indian, and south Pacific oceans. In Kovach, R.L. and Nur, A. (eds), *Proceedings of the conference on tectonic problems of the San Andreas Fault System*. Stanford, CA: Stanford University Press, 314–24.

Avouac, J.P. and Tapponnier, P., 1993. Kinematic model of active deformation in central Asia. *Geophysical Research Letters*, **20**: 895–98.

Bishop, M.P., Shroder, J.F., Bonk, R. and Olsenholler, J., 2002. Geomorphic change in high mountains: a western Himalayan perspective. *Global and Planetary Change*, **32**: 311–29.

Blisniuk, P.M., Hacker, B.R., Glodny, J., Ratschbacher, L., Siwan B., Zhenhan W., McWilliams, M.O. and Calvert, A., 2001. Normal faulting in central Tibet since at least 13.5 Myr ago. *Nature*, **412**: 628–32.

Brown, R.W., Gallagher, K., Gleadow, A.J.W. and Summerfield, M.A., 2000. Morphotectonic evolution of the South Atlantic margins of Africa and South America. In Summerfield, M.A. (ed.), *Geomorphology and global tectonics*. Chichester: Wiley, 255–82.

Burbank, D., Leland, J., Fielding, E., Anderson, R.S., Brozovik, N., Reid, M.R. and Duncan, C., 1996. Bedrock incision, rock uplift and threshold hillslopes in the northwestern Himalaya. *Science*, **276**: 571–74.

Chang Hui-Cheng (ed.), 2000. *Geological studies of the Chi-Chi (921) earthquake*. Taipei: Central Geological Survey.

Chen, W.P. and Kao, H., 1996. Seismotectonics of Asia: some recent progress. In Yin, A. and Harrison M. (eds), *The tectonic evolution of Asia*. New York: Cambridge University Press, 37–62.

Chen, W.P., Chen, C.Y. and Nabelek, J.L., 1999. Present-day deformation of the Qaidam Basin with implications for intra-continental tectonics. *Tectonophysics*, **305**: 165–81.

Chen, Z., Burchfield, B.C., Liu, Y., King, R.W., Royden, L.H., Tang, W., Wang, E., Zhao, J. and Zhang, X., 2000. Global positioning system measurements from eastern Tibet and their implications for India–Eurasia intercontinental deformation. *Journal of Geophysical Research*, **105**: 16215–27.

Chung, S.L., Lo, C.H., Lee, T.Y., Zhang, Y., Xie, Y., Li, X., Wang, K.L. and Wang, P.L., 1998. Diachonous uplift of the Tibet Plateau starting 40 Myr ago. *Nature*, **394**: 769–73.

Coleman, M. and Hodges, K., 1995. Evidence for Tibetan Plateau uplift before 14 Myr ago from a new minimum age for east-west extension. *Nature*, **374**: 49–52.

Collette, B.J., 1986. Fracture zones in the North Atlantic: morphology and a model. *Journal of the Geological Society of America*, **143**: 763–74.

Coney, P.J., 1987. The regional tectonic setting and possible causes of Cenozoic extension in the North America Cordillera. In Coward, M.P., Dewey, J.F. and Hancock, P.L. (eds), *Continental extensional tectonics*. Geological Society Special Publication 28. London: Geological Society of London, 177–86.

Coward, M.P., Butler, R.W.H., Khan, M.A. and Knipe, R.J., 1987. The tectonic history of Kohistan and its implications for Himalayan structure. *Journal of the Geological Society of London*, **144**: 377–91.

Cox, B.F., Hillhouse, J.W. and Owen, L.A., 2003. Pliocene and Pleistocene evolution of the Mojave River, and associated tectonic development of the Transverse Ranges and Mojave Desert, based on borehole stratigraphy studies and mapping of landforms and sediments near Victorville, California. In Enzel, Y., Wells, S. and Lancaster, N. (eds), *Paleoenvironment and paleohydrology of the Mojave and southern Great Basin deserts*. Geological Society of America Special Paper, 368, pp. 1–42.

Csejtey, B., Cox, D.P., Evarts, R.C., Stricker, G.D. and Foster, H.L., 1982. The Cenozoic Denali fault system and the Cretaceous accretionary development of southern Alaska. *Journal of Geophysical Research*, **87**: 3742–54.

Cunningham, W.D., Windley, B.F., Dorjnamjaa, D., Badamgarov, G. and Saander, M., 1996. Late Cenozoic transpression in southwestern Mongolia and the Gobi Altai-Tien Shan connection. *Earth and Planetary Science Letters*, **140**: 67–82.

Debon, F., Le Fort, P., Sheppard, S.M.F. and Sonet, J., 1986. The four plutonic belts of the Transhimalaya–Himalaya: a chemical, mineralogical and chronological synthesis along a Tibet–Nepal section. *Journal of Petrology*, **27**: 219–50.

DeMets, C., Gordon, R.G., Argus, D.F. and Stein, S., 1994. Effect of recent revisions to the geomagnetic reversal time scale on estimates of current plate motion. *Geophysical Research Letters*, **21**: 2191–94.

Dewey, J.F., Pitman, III, W.C., Ryan, W.B.F. and Bonnin, J., 1973. Plate tectonics and the evolution of the Alpine system. *Geological Society of America Bulletin*, **84**: 3137–80.

Dilek, Y. and Moores, E.M., 1999. A Tibetan model for the early Tertiary western United States. *Journal of the Geological Society of London*, **156**: 929–41.

Ellis, S., 1996. Forces driving continental collision: reconciling indentation and mantle subduction tectonics. *Geology*, **24**: 699–702.

England, P. and Houseman, G., 1989. Extension during continental convergence, with application to the Tibetan Plateau. *Journal of Geophysical Research*, **94**: 17561–69.

England, P. and McKenzie, D.P., 1982. A thin viscous sheet model for continental deformation. *Geophysical Journal of the Royal Astronomical Society*, **70**: 295–321.

England, P. and Searle, M.P., 1986: The Cretaceous–Tertiary deformation of the Lhasa block and its implications for crustal thickening in Tibet. *Tectonics*, **5**: 1–14.

Gilchrist, A.R. and Summerfield, M.A., 1990. Differential denudation and flexural isostasy in formation of rifted margin upwarps. *Nature*, **346**: 739–42.

Gilchrist, A.R. and Summerfield, M.A., 1994. Tectonic models of passive margin evolution and their implications for theories of long-term landscape development. In Kirkby, M.J. (ed.), *Process models and theoretical geomorphology*. Chichester: Wiley, 55–84.

Gilchrist, A.R., Summerfield, M.A. and Cockburn, H.A.P., 1994. Landscape dissection, isostatic uplift, and the morphologic development of orogens. *Geology*, **22**: 963–66.

Gregory, K.M. and Chase, C.G., 1992. Tectonic significance of paleobotanically estimated climate and altitude of the late Eocene erosion surface. *Geology*, **20**: 581–85.

Gudmundsson, A., 2000. Dynamics of volcanic systems in Iceland: example of tectonism and volcanism at juxtaposed hot spot and mid-ocean ridge systems. *Annual Review of Earth and Planetary Sciences*, **28**: 107–40.

Gunnell, Y. and Fleitout, L., 2000. Morphotectonics evolution of the Western Ghats, India. In Summerfield, M.A. (ed.), *Geomorphology and global tectonics*. Chichester: Wiley, 321–38.

Hamilton, W.B., 1988. Laramide crustal shortening. In Schmidt, C.J. and Perry, W.J. (eds), Interaction of the Rocky Mountain Foreland and the Cordilleran Thrust Belt. *Geological Society of America Memoirs*, **171**: 27–39.

Harbor, J. and Warburton, J., 1992. Glaciation and denudation rates. *Nature*, **356**: 751.

Harrison, T.M., Copeland, P., Kidd, W.S.F. and Yin, A., 1992. Raising Tibet. *Science*, **255**: 1663–70.

Harrison, T.M., Yin, A. and Ryerson, F.J., 1998. Orographic evolution of the Himalaya and Tibetan plateau. In Crowley, T.J. and Burke, K.C. (eds), *Tectonic boundary conditions for the climate reconstruction*. New York: Oxford University Press, 21–71.

Hatcher, R. and Williams, R.T., 1986. Mechanical model for single thrust sheets. *Geological Society of America Bulletin*, **97**: 975–85.

Hendix, M.S., Dumitru, T.A. and Graham, S.A., 1994. Late Oligocene–early Miocene unroofing in the Chinese Tien Shan: an early effect of the India–Asia collision. *Geology*, **22**: 487–90.

Holt, W.E., Li, M. and Haines, A.J., 1995. Earthquake strain rates and instantaneous relative motions within central and eastern Asia. *Geophysical Journal International*, **122**: 569–93.

Houseman, G. and England, P., 1996. A lithospheric thickening model for the Indo-Asian collision. In Yin, A. and Harrison, T.M. (eds), *The tectonic evolution of Asia*. New York: Cambridge University Press, 3–17.

Hsu, K.J., 1995. *The geology of Switzerland: an introduction to tectonic facies*. Princeton, NJ: Princeton University Press.

Hsu, K.J., Sengor, A.M.C., Briegel, U., Chen, H., Chen, C., Harris, N., Hsu, P., Li, J., Luo, J., Typhon, L., Li, Z.X., Chiayu, L., Powell, C., Wang, Q. and Winterer, E.L., 1995. Tectonic evolution of the Tibetan Plateau: a working hypothesis based on the archipelago model of orogenesis. *International Geological Reviews*, **37**: 473–508.

Hurtado, J.M., Hodges, K.V. and Whipple, K.X., 2001. Neotectonics of the Thakkhola graben and implications for recent activity on the South Tibetan fault system in the central Himalaya. *Geological Society of America Bulletin*, **113**: 222–40.

Jaillard, E., Soler, P., Carlier, G. and Mourier, T., 1990. Geodynamic evolution of the northern and central Andes during early to middle Mesozoic times: a Tethyan model. *Journal of the Geological Society of London*, **147**: 1009–22.

Jordan, T.E., Isacks, B.L., Allmendinger, R.W., Brewer, J.A., Ramos, V.A. and Ando, C.J., 1983. Andean tectonics related to geometry of subducted Nazca plate. *Geological Society of America Bulletin*, **94**: 341–61.

Kay, S.M., Mpodozis, C., Ramos, V.A. and Munizaga, F., 1991. Magma source variations for mid–late Tertiary magmatic rocks associated with a shallowing subduction zone and a thickening crust in the central Andes (28–33°S). *Geological Society of America Special Paper*, **265**: 113–37.

King, P.B., 1977. *Evolution of North America*. Princeton, NJ: Princeton University Press.

King, R.W., Shen, F., Burchfield, B.C., Royden, L.H., Wang, E., Chen, Z., Liu, Y., Zhang, X., Zhao, J. and Li, Y., 1997. Geodetic measurement of crustal motion in southwest China. *Geology*, **25**: 1279–82.

Larson, K., Burgmann, R., Billham, R. and Freymueller, J.T., 1999. Kinematics of the India–Eurasian collision zone from GPS measurements. *Journal of Geophysical Research,* **104**: 1077–94.

Laubscher, H.P., 1982. Detactment, shear, and compression in the central Alps. *Geological Society of America Memoir*, **158**: 191–211.

Lee, C.T. and Wang, Y., 1987. Palaeostress change due to the Pliocene–Quaternary arc-continent collision in Taiwan. *Memoir of the Geological Society of China*, **9**: 63–86.

Li, Y.H., 1976. Denudation of Taiwan Island since the Pliocene Epoch. *Geology*, **4**: 105–107.

Lin, J.C., 1991. The structural landforms of the Coastal Range of eastern Taiwan. In Cosgrove, J. and Jones, M. (eds), *Neotectonics and resources*. London: Belhaven Press, 65–74.

Lin, J.C., 2000. Morphotectonic evolution of Taiwan. In Summerfield, M.A. (ed.), *Geomorphology and global tectonics*. Chichester: Wiley, 135–46.

Love, J.D. and Reed, J.C., 1971. *Creation of the Teton landscape, the geologic story of the Grand Teton National Park*. Moose, WY: Grand Teton Natural History Association.

Lui, M., Shen, Y. and Yang, Y., 2000. Gravitational collapse of orogenic crust: a preliminary three-dimensional finite element study. *Journal of Geophysical Research*, **105**: 3159–73.

Macdonald, K.C., 1982. Mid-ocean ridges: fine scale tectonic, volcanic and hydrothermal processes within the plate boundary zone. *Annual Review of Earth and Planetary Science*, **10**: 155–90.

Mattauer, M., 1986. Intracontinental subduction, crust–mantle decollement and crustal-stacking wedge in the Himalayas and other collision belts. In Coward, M.P. and Ries, A.C. (eds), *Collision tectonics*. Geological Society Special Publication, 19. London: Geological Society of London 37–50.

Maxwell, J.C., 1974. Anatomy of an orogen. *Geological Society of America Bulletin*, **85**: 1195–204.

McCourt, W.J., Aspden, J.A. and Brook, M., 1984. New geological and geochronological data from the Colombian Andes: continental growth by multiple accretion. *Journal of the Geological Society of London*, **141**: 831–45.

Megard, F., 1989. The evolution of the Pacific Ocean margin in South America north of the Africa elbow (18˚S). In Ben-Avrahem, Z. (ed.), *The evolution of the Pacific Ocean margins*. New York: Oxford University Press, 208–30.

Molnar, P. and England, P., 1990. Late Cenozoic uplift of mountain ranges and global climate change: chicken or egg? *Nature*, **346**: 29–34.

Molnar, P. and Tapponnier, P., 1975. Cenozoic tectonics of Asia: effects of a continental collision. *Science*, **189**: 419–26.

Molnar, P. and Tapponnier, P., 1978. Active tectonics in Tibet. *Journal of Geophysical Research*, **85**: 5361–75.

Montgomery, D.R. 1994. Valley incision and the uplift of mountain peaks. *Journal of Geophysical Research*, **99**: 913–21.

Moores, E.M. and Twiss, R.J., 1995. *Tectonics*. New York: W.H. Freeman and Company.

Mpodozis, C. and Ramos, V., 1989. The Andes of Chile and Argentina. In Erickson, G.E., Canas, P.M.T. and Reinemund, J.A. (eds), *Geology of the Andes and its relation to hydrocarbon and mineral resources*. Houston, TX: Circum-Pacific Council for Energy and Mineral Resources Earth Science Series.

Murphy, M.A., Yin, A., Harrision, T.M., Durr, S.B., Chen, Z., Ryerson, F.J., Kidd, W.S.F., Wang, X. and Zhou, X., 1997. Did the Indo-Asian collision alone create the Tibetan plateau? *Geology*, **25**: 719–22.

Nelson, K.D., Zhao, W., Brown, L.D., Kuo, J., Che, J., Liu, X., Klemperer, S.L., Makovosky, Y., Meissner, R., Mechie, J., Kind, R., Wenzel, F., Ni, J., Nabelek, J., Leshou, C., Tan, H., Wei, W., Jones, A.G., Brooker, J., Unsworth, M., Kidd, W.S.F., Huack, M., Alsdorf, D., Ross, A., Rogan, M., Wu, C., Sandvol, E. and Edwards, M., 1996. Partially molten middle crust beneath southern Tibet: synthesis of project INDEPTH results. *Science*, **274**: 1684–88.

Nicholas, A., 1995. *The mid-oceanic ridges: mountains below sea level.* Berlin: Springer-Verlag.

Owens, T.J. and Zandt, G., 1997. Implications of crustal property variations for models of Tibetan plateau evolution. *Nature*, **387**: 37–43.

Patriat, P. and Achache, J., 1984. India–Eurasia collision chronology has implications for crustal shortening and driving mechanism of plates. *Nature*, **311**: 615–21.

Peltzer, G. and Tapponnier, P., 1988. Formation and evolution of strike-slip faults, rifts, and basins during the India–Asia collision: an experimental approach. *Journal of Geophysical Research*, **93**: 15085–117.

Petterson, M.G. and Windley, B.F., 1985. Rb-Sr dating of the Kohistan batholith in the Trans-Himalaya of North Pakistan, and tectonic implications. *Earth and Planetary Science Letters*, **74**: 45.

Pierce, K.L. and Morgan, L.A., 1992. The track of the Yellowstone hot spot: volcanism, faulting and uplift. *Geological Society of America Memoir*, **179**: 1–53.

Potter, C.J., Sanford, W.E., Yoos, T.R., Prussen, E.I., Keach, II, R.W., Oliver, J.E., Kaufman, S. and Brown, L.D., 1986. COCORP transect of the Washington–Idaho Cordillera. *Tectonics*, **5**: 1007–26.

Ramos, V.A., 1988. Late Proterozoic–early Palaeozoic of South America. *Episodes*, **11**: 168–74.

Ramstein, G., Fluteau, F.F., Besse, J. and Joussaume, S., 1997. Effect of orogeny, plate motion, and land–sea distribution on Eurasian climate over the past 30 million years. *Nature*, **286**: 788–95.

Raymo, M.E. and Ruddiman, W.F., 1992. Tectonic forcing of late Cenozoic climate. *Nature*, **359**: 117–22.

Reading, H.G. and Mitchell, N.C., 2000. Mid-ocean ridges. In Hancock, P.L. and Skinner, B.J. (eds), *The Oxford companion to the Earth*. Oxford: Oxford University Press, 683–87.

Reuber, I., 1989. The Dras arc: two successive volcanic events in eroded oceanic crust. *Tectonophysics*, **161**: 93–106.

Roeder, D.H., 1977. Continental convergence in the Alps. *Tectonophysics*, **40**: 339–50.

Roeder, D.H., 1988. Andean-age structure of eastern Cordillera (Province of La Paz, Bolivia). *Tectonics*, **7**: 23–40.

Roeder, D.H. and Mull, C.G., 1978. Ophiolites of the Brooks Range. *American Association of Petroleum Geologists Bulletin*, **62**: 1692–702.

Ruddiman, W.F., 1997. *Tectonic uplift and climate change*. New York: Plenum Press.

Ruddiman, W.F., 1998. Early uplift in Tibet? *Nature*, **394**: 723–35.

Ruddiman, W.F. and Kutzbach, J.E., 1989. Forcing of Late Cenozoic northern hemisphere climate by plateau uplift in southern Asia and the American west. *Journal of Geophysical Research*, **94**: 18409–27.

Ryan, P.D., 2000. Alpine orogeny. In Hancock, P.L. and Skinner, B.J. (eds), *The Oxford companion to the Earth*. Oxford: Oxford University Press, 14–16.

Schneider, D.A., Edwards, M.A., Kidd, W.S.F., Khan, M.A., Seeber, L. and Zeitler, P.K., 1999. Tectonics of Nanga Parbat, western Himalaya: synkinematic plutonism within the double vergent shear zones of crustal-scale pop-up structure. *Geology*, **27**: 999–1002.

Searle, M.P., 1991. *Geology and tectonics of the Karakoram Mountains*. Chichester: Wiley.

Searle, M.P. and Owen, L.A., 1999. The evolution of the Indus River in relation to topographic uplift, erosion, climate and geology of western Tibet, the Transhimalayan and High Himalayan Ranges. In Meadows, A. and Meadows, P. (eds), *The Indus River*. Oxford: Oxford University Press, 210–30.

Sengor, A.M.C. and Natal'in, B.A., 1996. Paleotectonics of Asia: fragments of a synthesis. In Yin, A. and Harrison, M. (eds), *The tectonics of Asia*. New York: Cambridge University Press, 486–640.

Seno, T., 1977. The instantaneous rotation vector of the Philippine Sea Plate relative to the Eurasian Plate. *Tectonophysics*, **42**: 209–26.

Shroder, Jr, J.F. and Bishop, M.P., 2000. Unroofing of the Nanga Parbat Himalaya. In Khan, M.A., Treloar, P.J., Searle, M.P. and Jam, M.Q. (eds), *Tectonics of the Nanga Parbat Syntaxis and the Western Himalaya*. Geographical Society Special Publication, 170. London: Geological Society of London, 163–79.

Speed, R., Ellison, M.W. and Heck, F.R., 1988. Phanerozoic tectonic evolution of the Great Basin. In Ernst, W.G. (ed.), *Metamorphism and crustal evolution of the Western United States*. Ruby Volume VII. Englewood Cliffs NJ: Prentice Hall, 572–605.

Sullivan, M.A., Windley, B.F., Saunders, A.D., Haynes, J.R. and Rex, C.C., 1993. A palaeogeographic reconstruction of the Dir Group: evidence for magmatic arc migration within Kohistan, N. Pakistan. In Treloar, P.J. and Searle, M.P. (eds), *Himalayan tectonics*. Geographical Society Special Publication, 74. London: Geological Society of London 139–60.

Summerfield, M.A., 1991a. *Global geomorphology*. London: Longman.

Summerfield, M.A., 1991b. Sub-aerial denudation of passive margins: regional elevation versus local relief models. *Earth and Planetary Science Letters*, **102**: 460–69.

Tapponnier, P. and Molnar, P.J., 1976. Slip-line field theory and large-scale continental tectonics. *Nature*, **264**: 319–24.

Tapponnier, P., Peltzer, G. and Armijo, R., 1986. On the mechanics of the collision between India and Asia. In Coward, M.P. and Ries, A.C. (eds), *Collision tectonics*. Geographical Society Special Publication, 19. London: Geological Society of London, 115–57.

Thompson, G.A. and Burke, D.B., 1974. Regional geophysics of the Basin and Range province. *Annual Reviews of Earth and Planetary Sciences*, **2**: 213–38.

Tippett, J.M. and Hovius, N., 2000. Geodynamic processes in the Southern Alps, New Zealand. In Summerfield, M.A. (ed.), *Geomorphology and global tectonics*. Chichester: Wiley, 109–34.

Troll, C., 1973a. The upper timberlines in different climatic zones. *Arctic and Alpine Research*, **5**: 3–18.

Troll, C., 1973b. High mountain belts between the polar caps and the equator: their definition and lower limit. *Arctic and Alpine Research*, **5**: 19–21.

Uyeda, S., 1978. *The new view of the Earth*. San Francisco, CA: W.H. Freeman and Company.

Vicente, J.-C., 1989. Early late Cretaceous overthrusting in the western Cordillera of southern Peru. In Erickson, G.E., Canas, P.M.T. and Reinemund, J.A. (eds), *Geology of the Andes and its relation to hydrocarbon and mineral resources*. Houston, TX: Circum-Pacific Council for Energy and Mineral Resources Earth Science Series, Volume 11.

Vilotte, J.P., Daignieres, M. and Madariaga, R., 1982. Numerical modeling of intraplate deformation: simple mechanical models of continental collision. *Journal of Geophysical Research*, **87**: 19709–28.

Vogt, P.R., 1981. On the applicability of thermal conduction models to mid-plate volcanism; comments on a paper by Gass *et al. Journal of Geophysical Research*, **86**: 950–60.

Wang, C.-H. and Burnett, W.C., 1991. Holocene mean uplift rates across an active plate-collision boundary in Taiwan. *Science*, **248**: 204–206.

Wang, M., Shen, Z.K., Jackson, D., Yin, A., Li, Y., Zhao, C., Dong, D. and Fang, P., 1999. GPS-derived deformation along the northern rim of the Tibetan Plateau and southern Tarim basin. *EOS, Transactions of the American Geophysical Union*, **80**: F1009.

Watts, A.B. and ten Brink, U.S., 1989. Crustal structure, flexure and subsidence history of the Hawaiian Islands. *Journal of Geophysical Research*, **94**: 10473–500.

Whipple, K.X. and Tucker, G.E., 1999. Dynamics of the stream-power river incision model: implications for height limits of mountain ranges, landscape response timescales, and research needs. *Journal of Geophysical Research*, **104**: 17661–74.

Whittington, A.G., 1996. Exhumation overrated. *Tectonophysics*, **206**: 215–26.

Wolfe, J.A., Schorn, H.E., Forest, C.E. and Molnar, P., 1997. Paleobotanical evidence for high altitudes in Nevada during the Miocene. *Nature*, **276**: 1672–75.

Wu, C., Nelson, K.D., Wortman, G., Samson, S.D., Yue, Y., Li, J., Kidd, W.S.F. and Edwards, M.A., 1998. Yadong cross structure and South Tibetan detachment in the east central Himalaya (89°–90°E). *Tectonics*, **17**: 28–45.

Yang, Y. and Liu, M., 2000. The rise and fall of the Tibetan Plateau: results of 3D numeric modelling. *EOS, Transactions of the American Geophysical Union*, **80**: F1230.

Yin, A., 2000. Modes of Cenozoic east–west extension in Tibet suggesting a common origin of rifts in Asia during the Indo-Asian collision. *Journal of Geophysical Research*, **105**(B9): 21745–59.

Yin, A. and Harrison, T.M., 2000. Geologic evolution of the Himalayan–Tibetan orogen. *Annual Reviews of Earth and Planetary Sciences*, **28**: 211–80.

Yin, A., Kapp, P.A., Murphy, M.A., Manning, C.E., Harrison, T.M., Grove, M., Ding, L., Deng, X. and Wu, C., 1999. Significant late Neogene east–west extension in northern Tibet. *Geology*, **27**: 787–90.

Zeitler, P.K., Meltzer, A.S., Koons, P.O., Craw, D., Hallet, B., Chamberlain, C.P., Kidd, W.S.F., Park, S.K., Seeber, L., Bishop, M. and Shroder, J., 2001. Erosion, Himalayan geodynamics and the geomorphology of metamorphism. *GSA Today*, January: 4–9.